Med Ultrason 2024, Vol. 26, no. 1, 97-107

Ultrasonography in plantar fibromatosis: the conduit between heel pain and 'catwalk'

Mahmud Fazıl Aksakal[1], Ahmad J. Abdulsalam[1,2], Ayşen Akıncı[1], Murat Kara[1], Levent Özçakar[1]

[1]Department of Physical and Rehabilitation Medicine, Hacettepe University Medical School, Ankara, Turkey,
[2]Department of Physical Medicine and Rehabilitation, Mubarak Alkabeer Hospital, Kuwait

To the Editor,

A 62-year-old woman presented with pain on the soles of her feet that had increased over the last two years. She reported that the pain was more severe in the morning and exacerbated by weight bearing. Her medical history revealed primary ovarian insufficiency in her 20s, for which she had received continuous combined hormone replacement therapy for over 10 years. In addition, the patient was a chronic/heavy ex-smoker (40 pack years) but had quit 15 years ago. Moreover, she had taken 0.5 mg of off-label alprazolam a few times a week for the past 10 years for her insomnia. The patient had no history of diabetes, epilepsy, Dupuytren's disease, alcohol, or trauma, and denied any family history of similar diseases.

Upon physical examination, two/small palpable tender lumps were detected on the medial plantar aspects of her feet. The insertions of both plantar fasciae were painless, with no contracture of the toes. Ultrasound examination using sono-palpation revealed bilateral elongated solid hypoechoic masses in the plantar fasciae 1.35×0.21×0.87 mm and 1.29×0.38×0.96 mm on the right and left feet, respectively (fig 1). Since the thickness and echogenicity of the plantar fasciae were normal on both calcaneal insertion sites, she was diagnosed with bilateral plantar fibromatosis. Ultrasound-guided intralesional corticosteroid injections were performed bilaterally. On the 1st week control visit, her complaints were significantly improved, and the mass lesions were reduced in size.

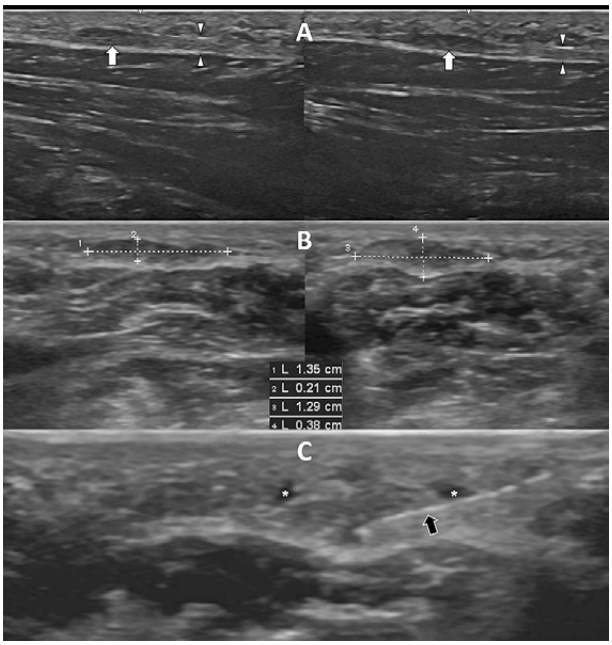

Fig 1. Comparative ultrasound imaging and measurements for the right and left plantar fasciae, respectively. Longitudinal (A) and axial (B) views show bilateral, elongated, solid hypoechoic masses *(white arrows)* and normal plantar fasciae *(arrowheads)*. Axial view of ultrasound-guided intralesional corticosteroid injection (C). Note the anechoic fluid *(asterisks)* leaking from the mass during the injection. *Black arrows:* needle.

Herein, we discuss a patient who presented with bilateral plantar fibromatosis after years of smoking, hormone replacement therapy, and benzodiazepine use. Plantar fibromatosis is a rare benign disease characterized by nodule formation comprising hyperproliferative fibrous tissue along the plantar fascia [1]. It can be associated with other conditions, such as Dupuytren's disease, dia-

Received 10.02.2024 Accepted 12.02.2024
Med Ultrason
2024, Vol. 26, No 1, 97-98, DOI: 10.11152/mu-4338,
Corresponding author: Ahmad Jasem Abdulsalam
Department of Physical Medicine
and Rehabilitation
Mubarak Alkabeer Hospital,
Jabriya, Kuwait
E-mail: dr.ahmad.j.abdulsalam@gmail.com

betes, alcohol use, and smoking. It has also been related with continuous phenobarbital treatment [2]. Hurst et al. first postulated that antiepileptic drug therapy caused decreased prostaglandin E which, in turn, might allow palmar myofibroblast contraction and lead to Dupuytren's disease [3]. However, no studies have reported a similar association with benzodiazepine use, which also/indeed decreases prostaglandin E production [4]. In addition, considering the possible use of anti-estrogenic medications in fibromatosis – whereby they inhibit TGF-beta expression, fibroblast proliferation/maturation and myofibroblast differentiation [5] - we believe that estrogen replacement therapy might have contributed to our patient's condition. Finally, the role of ultrasound imaging/guidance would be noteworthy for the diagnosis, interventional treatment, and close follow up in relevant cases.

References

1. Stewart BD, Nascimento AF. Palmar and plantar fibromatosis: a review. J Pathol Transl Med 2021;55:265-270.
2. Hurst LC, Badalmente MA, Makowski J. The pathobiology of Dupuytren's contracture: effects of prostaglandins on myofibroblasts. J Hand Surg 1986;11:18-22.
3. Fruscella P, Sottocorno M, Di Braccio M, et al. 1,5-Benzodiazepine tricyclic derivatives exerting anti-inflammatory effects in mice by inhibiting interleukin-6 and prostaglandinE(2)production. Pharmacol Res 2001;43:445-452.
4. Kuhn MA, Wang X, Payne WG, Ko F, Robson MC. Tamoxifen decreases fibroblast function and downregulates TGFβ2 in Dupuytren's affected palmer fascia. J Surg Res 2002;103:146-152.
5. Noble J. Connective tissue disorders: discussion. In: Oxley J, Janz D, Meinardi H, eds. Chronic Toxicity of Antiepileptic Drugs. New York, NY: Raven Press; 1983:169-173.

Lung cancer with bilateral internal jugular vein thrombosis

Fenglin Jiang[1], Jingjun Zhu[2]

[1]Department of Medical Ultrasound, [2]Department of Chest Surgery, Yanbian University Hospital, Yanji, Jilin, China

To the Editor,

In a 64-year-old woman with lung adenocarcinoma, chest enhanced computed tomography (CT) showed a nodular shadow in the apical segment of the upper lobe of the right lung, with a size of approximately 2.0×1.6 cm, uneven enhancement, and multiple enlarged lymph nodes in the mediastinum. The results of fiberoptic bronchoscopy and pathological examination showed a small amount of atypical cell clusters under the mucosa, including CK7 (+), TTF-1 (+), P40 (-), and P63 (-). CA-125 102.90 U/mL, CEA 42.72 ng/mL, PLT 314x109/L, D-dimer 3.06 ug/ml. Internal jugular vein ultrasound examination showed bilateral internal jugular vein thrombosis (fig 1). MRI showed high signal on T2WI and low signal on T1WI in bilateral jugular veins, confirming bilateral internal jugular vein thrombosis.

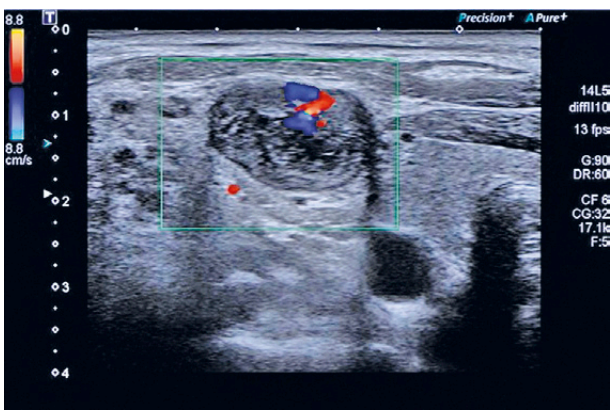

Fig 1. Ultrasound examination of the right internal jugular vein showed that the longitudinal section of the internal jugular vein is almost filled with hypoechoic light masses, indicating internal jugular vein thrombosis.

Internal jugular vein thrombosis is an extremely rare vascular disease. Patients with cancer are at increased risk for venous thromboembolism, and 8% to 15% of patients

Received 19.11.2023 Accepted 25.11.2023
Med Ultrason
2024, Vol. 26, No 1, 98-99, DOI: 10.11152/mu-4339,
Corresponding author: Fenglin Jiang
Department of Medical Ultrasound,
Yanbian University Hospital,
#1327 Juzi St., Yanji 133000, China
Phone: +86-433-2660056
E-mail: jiangfenglin@sina.com

with advanced non-small-cell lung cancer experience a venous thromboembolism event during the course of their disease. Venous thromboembolism events consisted of pulmonary embolism (46.4%), deep vein thrombosis (39.2%), renal vein thrombosis (7.1%), internal jugular vein thrombosis (3.5%), and peripheral inserted central catheter-related thrombosis (3.5%). Venous thromboembolism events occurred at disease progression in 35.7% of cases, at diagnosis in 32.1% of cases, and during chemotherapy in 17.8% [1]. Clinically relevant clotting abnormalities in cancer patients are referred to as Trousseau's syndrome [2]. Trousseau's syndrome (cancer-associated thrombosis) is the second leading cause of death in cancer patients, after death from cancer itself. The risk of a venous thromboembolism is 4- to 7-fold higher in patients with cancer than in those without cancer [3].

References

1. Chiari R, Ricciuti B, Landi L, Morelli AM, Delmonte A, Spitaleri G, et al. ROS1-rearranged Non-small-cell Lung Cancer is Associated With a High Rate of Venous Thromboembolism: Analysis From a Phase II, Prospective, Multicenter, Two-arms Trial (METROS). Clin Lung Cancer 2020;21:15-20.
2. Dicke C, Langer F. Pathophysiology of Trousseau's syndrome. Hamostaseologie 2015;35:52-59.
3. Ikushima S, Ono R, Fukuda K, Sakayori M, Awano N, Kondo K. Trousseau's syndrome: cancer-associated thrombosis. Jpn J Clin Oncol 2016;46:204-208.

The ultrasonography and pathological features of primary hepatic pleomorphic undifferentiated sarcoma

Yuhan Bao[1], Qingkai Meng[2], Nina Qu[3]

[1]Department of Breast Surgery, The Second Hospital of Shandong University, Jinan, Shandong, [2]Binzhou Medical University, Yantai, Shandong, [3]Department of Ultrasound Medicine, Yuhuangding Hospital, Yantai

To the Editor,

A 79-year-old male presented with persistent fever for several days, with a peak body temperature of 39.1°C. Abdominal CT scan revealed multiple ill-defined, nodular low-density lesions within the liver. Laboratory investigations showed a white blood cell count of 37.59×10^9/L and a high-sensitivity C-reactive protein level of 272.57 mg/L. Based on the combined radiological features the preliminary diagnosis of hepatic abscess was made. However, a subsequent ultrasound examination displayed heterogeneous echogenicity within the liver, indicative of the characteristic "bull's eye sign", a small amount of blood flow perfusion was observed within the nodules, with heterogeneous echogenicity. Contrast-enhanced ultrasound (CEUS) revealed a "fast in, fast out" pattern within the nodules, with a distinct area of inadequate blood perfusion. The histopathological examination of the liver biopsy revealed intratumoral infiltration of neoplastic cells, comprising spindle cells, epithelioid cells, and a subset of inflammatory cells, demonstrating nuclear atypia, necrosis, and focal abscesses. Immunostaining showed positive expression of Heppar-1 in hepatic cells, minimal positivity for S-100, and CD68 expression, with slight positivity for vimentin. Furthermore, the proliferation index assessed by Ki67 staining was high at 60%. Based on the integrated immunohistochemical analysis, the diagnosis of undifferentiated pleomorphic sarcoma (UPS) was rendered (fig 1).

Hepatic UPS is exceedingly rare, since the abolition of the concept of malignant fibrous histiocytoma (MFH) in 2013 and its replacement by UPS, only seven cases of primary hepatic UPS have been documented. Hepatic primary UPS mainly occurs in Caucasian descent in the middle to elderly age groups [1]. The clinical features of hepatic UPS bear resemblance to those of hepatic abscess, and the imaging characteristics lack specificity. CEUS features can assist in the differential diagnosis of

Received 04.02.2024 Accepted 12.02.2024
Med Ultrason
2024, Vol. 26, No 1, 99-100, DOI: 10.11152/mu-4340,
Corresponding author: Yuhan Bao
Department of Breast Surgery,
Second Hospital of Shandong University,
Jinan, Shandong, China
Email: 17851313396@163.com

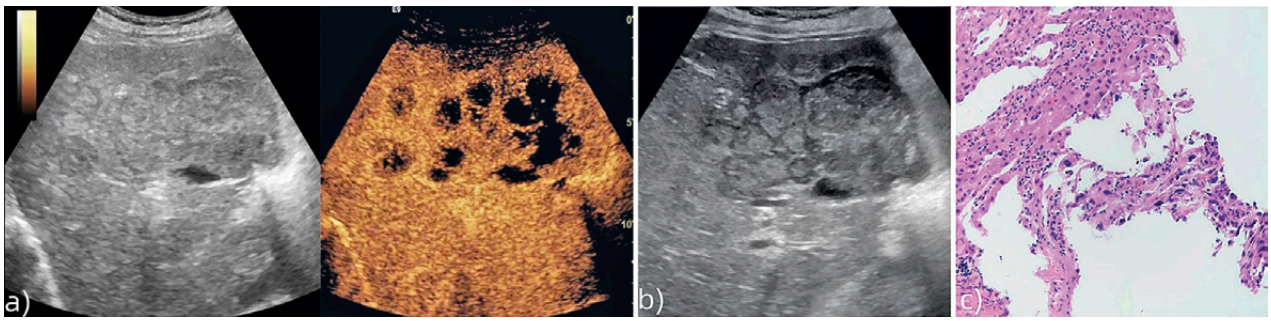

Fig 1. CEUS reveals heterogeneous enhancement of the lesion with associated areas of partial ischemic necrosis; b) 2D ultrasound showed heterogeneous echo in the liver with an area. Irregular shape, multiple nodules inside, like "bull's eye sign"; c) Biopsy pathology showed invasive growth of some tumor cells in the liver tissue, the tumor cells being mixed in composition, with mitotic figures, necrosis, and small abscess foci (HE×20).

these two conditions. CEUS scans reveal a "fast in and fast out" sign throughout the entire lesion, indicating a malignant tumor rather than a hepatic abscess. In clinical practice, when faced with patients exhibiting imaging features and clinical manifestations akin to hepatic abscess, and with a suboptimal response to anti-infective therapy, rare diseases such as UPS should be considered [2].

References

1. Kodera K, Hoshino M, Takahashi S, et al. Surgical management of primary undifferentiated pleomorphic sarcoma of the rectum: a case report and review of the literature. World J Surg Oncol 2022;20:199.
2. Wang Z, Xiao Y, Zhan, B, Xiaosong, Shao J, Liao J. Ultrasonographic diagnosis of primary hepatic undifferentiated pleomorphic sarcoma. J Clin Ultrasound 2023;51:169-176.

Right congenital pyriform sinus fistula

Wang Li, Yihua Gao

Department of Medical Ultrasound, Yanbian University Hospital, Yanji, China

To the Editor,

A 5-year-old boy was admitted to the hospital due to a right cervical mass. Physical examination showed a hard right cervical mass with poor mobility, tenderness, red and swollen surface skin, no ulceration, and inability to move up and down with swallowing. The ultrasound examination showed a mixed echo measuring approximately 24x12x18 mm in the lateral parapharyngeal region of the right thyroid lobe. This echo exhibited an irregular shape, multiple strong echo spots, uneven echo intensity, unclear boundary, and was further characterized by color Doppler flow imaging detecting point-like blood flow signals (fig 1a, b). Based on these findings, the lesion was diagnosed as a congenital pyriform sinus fistula (CPSF). Additionally, fiberoptic laryngoscopy revealed a fistula with a diameter of approximately 0.1 cm in the right pyriform sinus (fig 1c, d), thus confirming the diagnosis of CPSF.

CPSF is a rare disease of the neck and parotid gland, which is caused by the failure of the third or fourth branchial sac to degenerate during embryonic development [1]. It has been observed that approximately 93-97% of patients with CPSF develop the condition on the left side of the neck. Some scholars believe that this may be attributed to the degeneration or loss of the right branchial body and the asymmetric development of the fourth branchial arch [2]. Given its unique embryonic development and the complex local anatomical structure, early diagnosis of CPSF can be challenging. Previous studies have reported that the typical ultrasound appearance of CPSF manifests as a cystic mass with heteroge-

Received 22.12.2023 Accepted 10.01.2024
Med Ultrason
2024, Vol. 26, No 1, 100-101, DOI: 10.11152/mu-4341,
Corresponding author: Yihua Gao
Department of Medical Ultrasound, Yanbian University Hospital, Yanji 133000, China
E-mail: gyh20021997@163.com

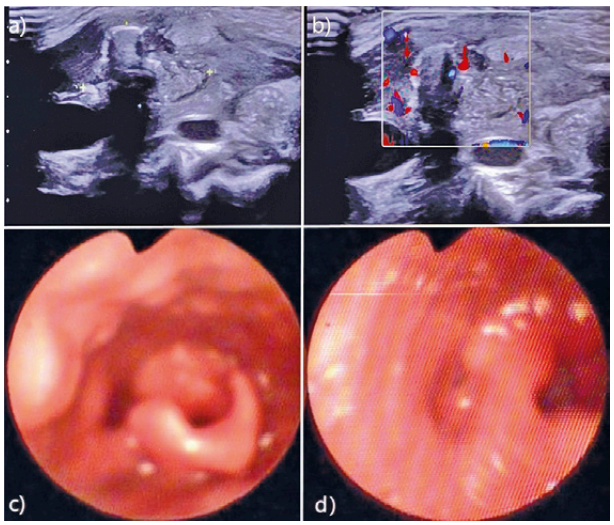

Fig 1. The ultrasound image shows a mixed echogenic mass with a size of about 24x12x18 mm (a, b). The fistula can be seen under fiberoptic laryngoscopy (c, d).

neous low-echo intensity in the neck, with poor internal echo penetration and the presence or absence of air in the lesion [3]. Additionally, ultrasound examination can clearly visualize the fistula and its direction, providing clinical guidance for surgical timing and evaluation of postoperative effects based on the varying ultrasound characteristics of CPSF during infection and non-infection periods.

References

1. Lin CY, Hsiao TY, Hsu WC. Pathognomonic ultrasonic images of congenital pyriform sinus fistula in Children. Clin Otolaryngol 2021;46:110-115.
2. Cain RB, Kasznica P, Brundage WJ. Right-sided pyriform sinus fistula: a case report and review of the literature. Case Rep Otolaryngol 2012;2012:934968.
3. Li L, Zhao DJ, Yao TY, et al. Imaging Findings in Neonates With Congenital Pyriform Sinus Fistula: A Retrospective Study of 45 Cases. Front Pediatr 2021;9:721128.

Ultrasound-guided thrombin injection in the management of brachial artery pseudoaneurysm with median nerve compression

Guoyun Wang[1], Jie Liu[2], Xiaoli Cao[1]

[1]Department of Ultrasound, The Affiliated Yantai Yuhuangding Hospital of Qingdao University, Yantai, [2]Department of Ultrasound, Rushan Traditional Chinese Medicine Hospital, Rushan, China

To the Editor,

An 85-year-old patient received a pacemaker implantation through percutaneous brachial artery approach due to arrhythmia. Ten days later, the patient suffered from pain at the puncture site of her left elbow, and her distal limb presented edema (fig 1A). The patient experienced numbness in her thumb, index, and middle fingers. Ultrasonic examination revealed a pseudoaneurysm (PSA) measuring approximately 3.5×1.9×1.9 cm at the puncture site of the left elbow, connected to the brachial artery, with a neck width of 2.5 mm. The sac exerted compression on the median nerve (fig 1B). Color Doppler flow imaging demonstrated red and blue blood signals within the sac. Contrast-enhanced ultrasound (CEUS) revealed lateral entry of contrast agent from the left brachial artery through the aneurysm cavity's neck into its interior (fig 1C).

Ultrasound-guided thrombin injection (UGTI) was performed by inserting a 22G needle into the PSA keeping away from the neck, then injecting 2 ml of thrombin solution (250 U/ml) into the sac and confirming that the PSA was completely thrombotic, and the distal artery was unobstructed (fig 1D, E). The sac volumes at 1, 2, 4, and 12 weeks follow-up assessment after UGTI were 6.55, 3.06, 0.77, and 0.07 cm^3 respectively, and the volume reduction rates measured at 0.3%, 53.2%, 88.2%, and 98.9% (fig 1F-I). Correspondingly, the symptoms of

Received 03.01.2024 Accepted 06.01.2024
Med Ultrason
2024, Vol. 26, No 1, 101-102, DOI: 10.11152/mu-4342,
Corresponding author: Xiaoli Cao
Department of Ultrasound,
The Affiliated Yantai Yuhuangding
Hospital of Qingdao University,
20 Yudong Road, Yantai,
Shandong 264000, China
E-mail: xiaolic969@163.com

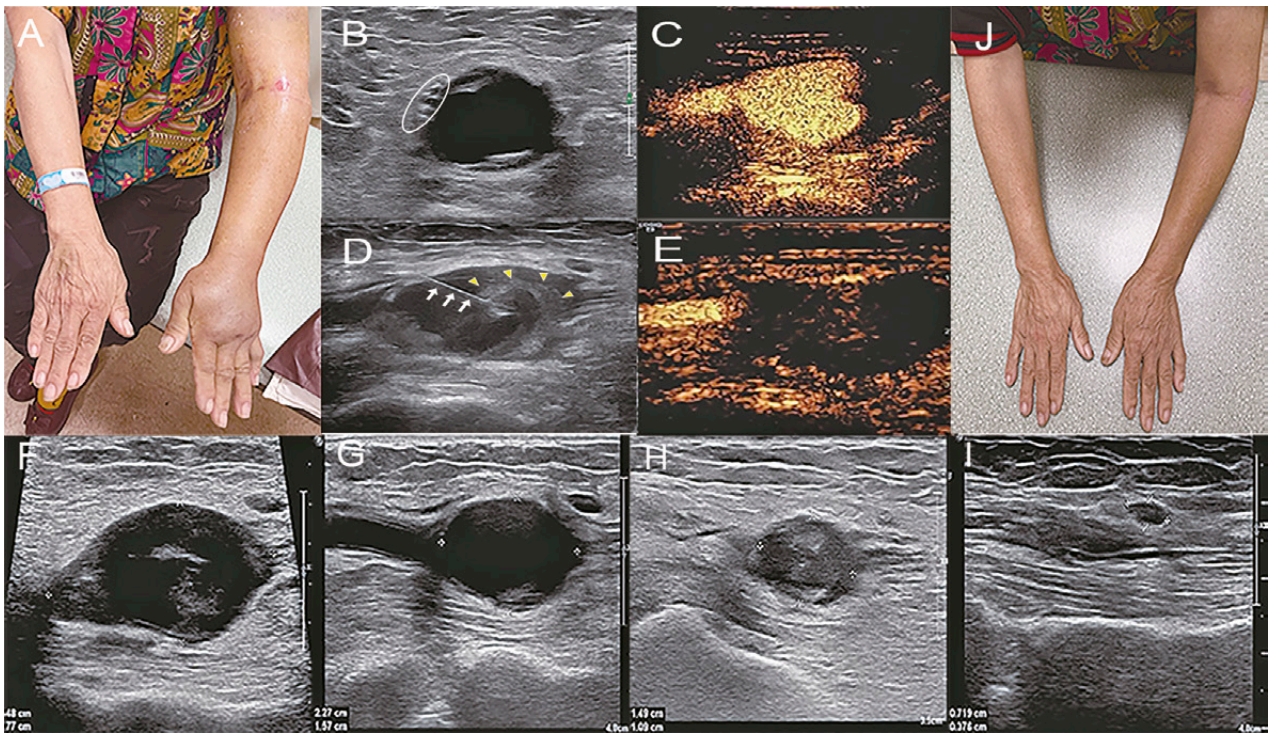

Fig 1. A. The left upper limb was more swollen and bloodstained than the opposite side before UGTI; B. The transverse section showed anechoic sac and nerve with compression (oval part); D. CEUS showed the contrast agent entered the left brachial artery and PSA interior; C. UGTI showed that the puncture needle (arrow) was located in the cavity and the flocculent echo (yellow arrow); E. CEUS showed no flow into the sac and only revealed the left brachial artery; F-I. The sac volumes at 1, 2, 4, and 12 weeks after UGTI were reduced; J. No obvious swelling in the left upper limb after 2 weeks.

edema and hand numbness were obviously relieved (fig 1J).

The recovery period of median nerve damage compressed by brachial artery PSA after surgical operation ranges from 2 months to 1 year [1-2]. However, early intervention with UGTI can delay sustained compression on the nerve and prevent further damage. Within a span of 3 months, the intervention approach achieves a nearly 100% absorption rate which offers minimal invasiveness and rapid recovery while achieving comparable outcomes to surgery. This option not only improves patients' quality of life but also provides an additional choice for patients who are not suitable for surgery.

Acknowledgement: the work was supported by the Shandong Provincial Natural Science Foundation General Project (Grant No. ZR2021MH398)

References

1. Villanueva AG, Ona IR, Oya AS. Median Nerve Compression Caused by Brachial PSA: Report of Two Cases and Review of the Literature. J Hand Microsurg 2016;8:109-110.
2. Graham B, Peljovich AE, Afra R, et al. The American Academy of Orthopaedic Surgeons Evidence-Based Clinical Practice Guideline on: Management of Carpal Tunnel Syndrome. J Bone Joint Surg Am 2016;98:1750-1754.

Prenatal sonographic findings in a case with bilateral Tessier number 7 cleft in first trimester

Zheng Feng Zhu, Jie Li, Zhao Yu Wang

Ultrasound Department, Zhengzhou University Third Hospital and Henan Province Women and Children's Hospital, Zhengzhou, China

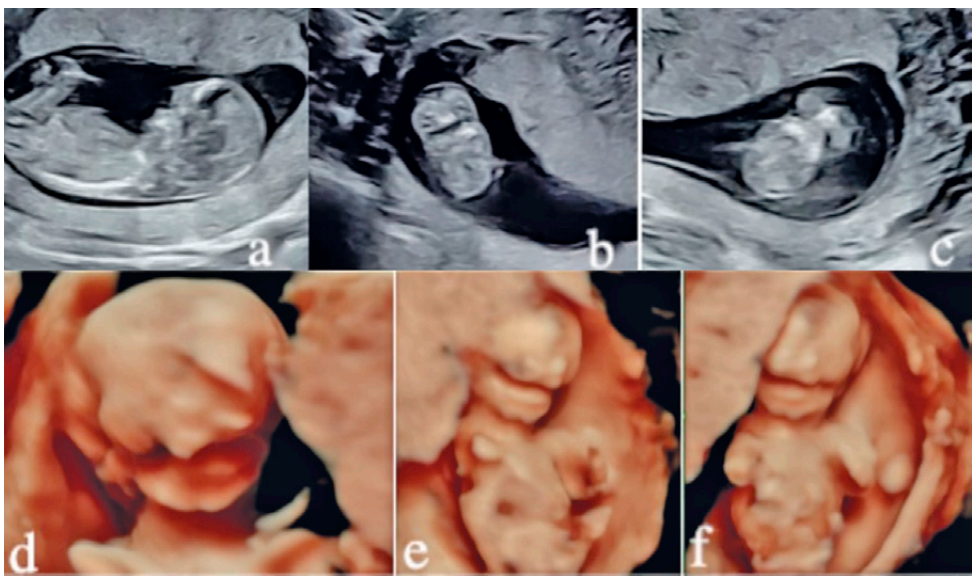

Fig 1. a) The 'superimposed-line' sign and vomer bone were absent; b) Macrostomia without morphological ears; c) Bilateral gap of the primary palate; d-f) Three-dimensional rendered surface.

To the Editor,

Macrostomia, also called transverse facial cleft, is characterized by a widening of the oral commissure, which is categorized as cleft number 7 according to Tessier's classification [1]. Various studies evaluation of macrostomia are common in the late pregnancy [2,3].

A 26-year-old G3P2 pregnant woman was referred to our center due to "abnormal fetal facial profile" with a crown-rump length of 59 mm. The facial profile demonstrated indiscernible nasal bridge and nasal bone with an almost absent maxilla in midsagittal view (Fig 1a); alveolar ridge was only partial and orofacial bilateral sulcus widening of the commissure of the mouth up to the position of the ears and with absent external ears (fig 1b) was present, while a bilateral gap existed in only part of the primary palate (fig 1c). Three-dimensional imaging of the face revealed bilateral transverse facial cleft accompanied with bilateral cleft palate (Fig1d-f). No other defect has been identified. The facial manifestations were consistent with the prenatal imaging when the fetus was induced.

Bilateral facial clefts are extremely rare. An abnormal facial profile was in the present case as we were unable to obtain the echogenic line representing the palate [4] or 'superimposed-line' sign [5]. With the evaluation of midsagittal, axial, and oblique coronal views, we considered macrostomia accompanied with bilateral cleft palate. Subsequently, the three-dimensional imaging of the face was intuitive. Three-dimensional ultrasound could provide superficial anatomical facial information about

Received 02.02.2024 Accepted 10.02.2024
Med Ultrason
2024, Vol. 26, No 1, 103-104, DOI: 10.11152/mu-4343,
Corresponding author: Zhengfeng Zhu
7 Kangfu Front Street, Erqi district,
ZhengZhou HeNan, China
E-mail: tiasny728g@163.com

the presence and severity of facial defects. We found an excellent correlation between the prenatal three-dimensional ultrasound and the postmortem appearance of the fetus. Hence, three-dimensional ultrasound can be valuable for lateral clefts during the first trimester.

References

1. Tessier P. Anatomical classification of facial cranio-facial and lateral-facial clefts. J Maxillofac Surg 1976;4:69-92.
2. Cavaco-Gomes J, Duarte C, Pereira E, Matias A, Montenegro N, Merz E. Prenatal ultrasound diagnosis of Tessier number 7 cleft: Case report and review of the literature. J Obstet Gynaecol 2017;37:421-427.
3. Lee M, Ko YB, Yang JB, Kang BH. Prenatal 3D sonography of an isolated lateral facial cleft. J Clin Ultrasound 2018;46:292-295.
4. Lakshmy SR, Rose N, Masilamani P, Umapathy S, Ziyaulla T. Absent 'superimposed-line' sign: novel marker in early diagnosis of cleft of fetal secondary palate. Ultrasound Obstet Gynecol 2020;56:906-915.
5. Chaoui R, Orosz G, Heling KS, et al. Maxillary gap at 11–13 weeks' gestation: Marker of cleft lip and palate. Ultrasound Obstet Gynecol 2015;46:665-669.

Early diagnosis of aspiration pneumonia by gastrointestinal ultrasound combined with lung ultrasound

Yaru Yan[1,2], Haotian Zhao[3], Ling Long[3], Chunyan Yang[1]

[1]Department of Ultrasound, Shijiazhuang People' Hospital, [2]Hebei Medical University, [3]Department of Ultrasound, Hebei General Hospital (Hebei General Hospital Affiliated to Hebei Medicine University), Shijiazhuang, Hebei, China

To the Editor,

Excessive gastric contents can lead to aspiration pneumonia when reflux occurs. Severe aspiration pneumonia can cause acute dyspnea. Early diagnosis of aspiration pneumonia can help save time and provide clear treatment directions.

A 61-year-old male was admitted to the emergency department for unidentified acute dyspnea. He was unable to remain in supine position due to shortness of breath with an oxygen saturation of 87% using pulse oximetry. Echocardiography showed a left ventricular ejection fraction of 70% and normal ventricular structure. The diameter of the inferior vena cava was 9.8 mm with a variation rate of 62.2%. No thrombus was found in the lower limb veins. Therefore, ultrasound (US) examination was considered to exclude cardiac dyspnea and pulmonary embolism.

Lung US showed consolidation in lung tissue of left lower back. The consolidation was not uniform, with a dendritic arrangement of bronchial structures visible inside (fig 1a). Hyperechoic material was seen in the bronchi which can flow with the patient's breathing movements. We considered it to be lung consolidation caused by pneumonia. The typical image of dynamic bronchogram indicated a mixture of gas and liquid flowing inside the bronchus. Scanning the probe along the left rib edge revealed a filled stomach (fig 1b). Uneven contents were seen in the stomach with no gastric antrum contraction over time (fig 1c), last meal being taken approximately 12 hours before examination and was interpreted as stomach retention. (delayed gastric emptying) Transient reflux occurred when the stomach pressure was high, leading to aspiration pneumonia. The patient subsequently underwent computer tomography (CT) examination and was diagnosed with pneumonia, which was consistent with lung US examination (fig 1d). As the condition progressed, the patient underwent emergency tracheal intubation and was transferred to the intensive care unit for treatment.

Consolidation is a common and important sign of lung US, which often occurs in pneumonia. Dynamic

Received 30.10.2023 Accepted 03.12.2023
Med Ultrason
2024, Vol. 26, No 1, 104-105, DOI: 10.11152/mu-4344,
Corresponding author: Chunyan Yang
Department of Ultrasound,
Shijiazhuang People' Hospital
36 Fanxi Road, Chang'an District,
Shijiazhuang, 050051 Hebei, China
E-mail: chunyancsk@126.com
Phone/fax: +086-0311-80915578
+086-0311-80915578

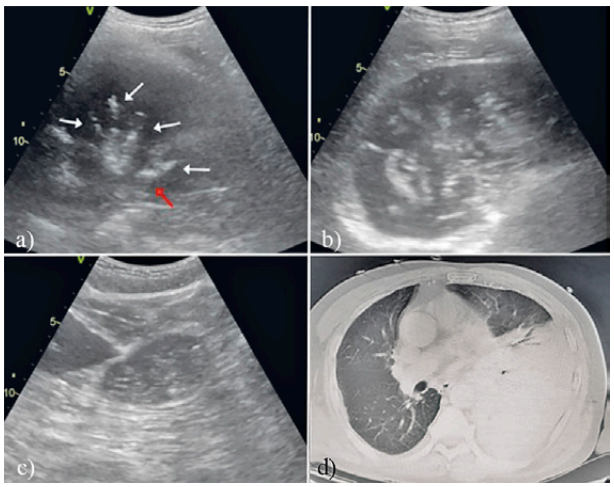

Fig 1. a) Ultrasound manifestations of lung consolidation, with dendritic bronchial structures (white arrow) and visible flow of gas inside (red arrow); b) Ultrasound shows large amount of gastric contents in the fundus of stomach; c) The gastric antrum is filled and its shape remains unchanged over time, indicating poor gastric antral contractile function; d) Chest computed tomography shows a large high density shadow in the left lower lung.

bronchogram is often present in exudative or aspiration pneumonia, while static bronchogram is often present in obstructive atelectasis [1]. Typical aspiration pneumonia can be seen on US as a dendritic arrangement of bronchial structures within the consolidation, and flow can occur with respiration. A significant amount of gastric residual volume is associated with the risk of aspiration [2]. When US reveals typical pneumonia, we can further slide the probe to observe the stomach. A smaller gastric volume can rule out aspiration pneumonia. However, when a larger stomach is found, we should be alert to the possibility of aspiration pneumonia.

References

1. Haaksma ME, Smit JM, Heldeweg MLA, et al. Extended Lung Ultrasound to Differentiate Between Pneumonia and Atelectasis in Critically Ill Patients: A Diagnostic Accuracy Study. Crit Care Med 2022;50:750-759.
2. Kruisselbrink R, Gharapetian A, Chaparro LE, et al. Diagnostic Accuracy of Point-of-Care Gastric Ultrasound. Anesth Analg 2019;128:89-95.

Ultrasonography and clinical findings of angiomyofibroblastoma in the right inguinal region

Xiaowei Zhang[1], Tingting Xu[1], Jiajia Ying[2]

[1]Department of Pathology, [2]Department of Surgical Center, Affiliated Dongyang Hospital of Wenzhou Medical University, Dongyang, Zhejiang, China

To the Editor,

A 33-year-old male patient was admitted with a right inguinal mass. The patient did not present with any swelling, pain, fever, nausea, or vomiting. On physical examination, the patient's abdomen was flat and soft, with no tenderness or rebound pain. We detected a mass approximately 4×3 cm near the center of the right inguinal furrow that did not reduce or disappear on palpation.

Subsequent ultrasonography revealed a 66×60×21mm hypoechoic mass in the subcutaneous tissue of the right groin, with clear boundaries and a non-uniform internal echo (fig 1a). Color Doppler flow imaging (CDFI) showed a thin-stripe blood flow signal. We surgically resected the right inguinal tumor. The immunohistochemical staining results were as follows: vimentin (+), SOX10 (-), S-100 (-), MSA (-), desmin (+), CD34 (+), MyoD1 (-), caldesmon (-), SMA (-), and Ki-67 (+, <1%) (fig 1b). Consequently, a postoperative histopathological diagnosis of right inguinal angiomyofibroblastoma (AMF) was established.

Received 30.01.2024 Accepted 01.02.2024
Med Ultrason
2024, Vol. 26, No 1, 105-106, DOI: 10.11152/mu-4328,
Corresponding author: Jiajia Ying
Department of Surgical Center,
Affiliated Dongyang Hospital
of Wenzhou Medical University,
No. 60 West Wuning Road, Dongyang,
Zhejiang, 322100, P.R. China
Phone/fax: +86 13967430313
+86 057989605211
E-mail: yjj20140725@163.com

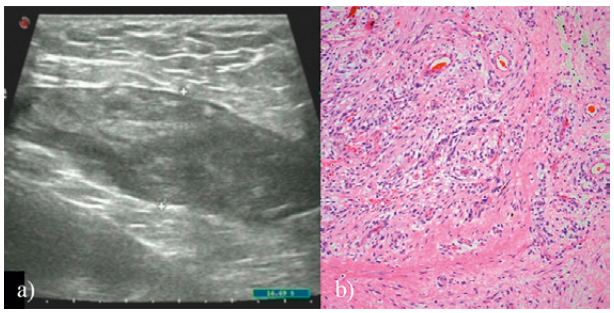

Fig 1. a) Ultrasound imaging indicating a hypoechoic mass in the subcutaneous tissue of the right groin. b) Non-atypical tumor cells clustered around the blood vessels (Hematoxylin and eosin stain × 100).

AMF is a rare and benign soft tissue tumor usually observed in the vulva or lower genital tract of young and middle-aged women, with few incidences in the male scrotum and groin. AMF can be cured with complete resection and has a good prognosis [1]. Owing to its convenience and ease in detecting surface body masses, ultrasound is preferred for the diagnosis of inguinal AMF. The preoperative ultrasound diagnosis of AMF in the groin should exclude other common benign and malignant lesions occurring in the groin [2]. AMF should be the primary diagnosis when the slow enlargement of painless masses in the inguinal furrow of young patients is observed on physical examination, and clear boundaries and non-uniform internal echo are observed on ultrasonography. In this patient, CDFI revealed a characteristic mass with abundant blood flow signals and a non-uniform internal echo.

References

1. Blel A, Mekni A, Bel Haj Salah M, et al. Paratesticular angiomyofibroblastoma: case report and review of the literature. Pathologica 2008;100:489-491.
2. Wolf B, Horn LC, Handzel R, Einenkel J. Ultrasound plays a key role in imaging and management of genital angiomyofibroblastoma: a case report. J Med Case Rep 2015;9: 248.

Ultrasound imaging of the transversus nuchae muscle: a potential entrapment site for the lesser occipital nerve

Federico Zaottini[1], Riccardo Picasso[1], Wei-Ting Wu[2, 3], Ke-Vin Chang[2,3,4], Kamal Mezian[5], Vincenzo Ricci[6], Levent Özçakar[7]

[1]Department of Radiology, IRCCS Policlinico San Martino, Genoa, Italy, [2]Department of Physical Medicine and Rehabilitation, National Taiwan University Hospital, Bei-Hu Branch, Taipei, Taiwan, [3]Department of Physical Medicine and Rehabilitation, National Taiwan University College of Medicine, Taipei, Taiwan, [4]Center for Regional Anesthesia and Pain Medicine, Wang-Fang Hospital, Taipei Medical University, Taipei, Taiwan, [5]Department of Rehabilitation Medicine, Charles University, First Faculty of Medicine and General University Hospital in Prague, Prague, Czech Republic, [6]Physical and Rehabilitation Medicine Unit, Luigi Sacco University Hospital, ASST Fatebenefratelli-Sacco, Milan, Italy, [7]Department of Physical and Rehabilitation Medicine, Hacettepe University Medical School, Ankara, Turkey

Received 05.11.2023 Accepted 25.11.2023
Med Ultrason
2024, Vol. 26, No 1, 106-107, DOI: 10.11152/mu-4345,
Corresponding author: Ke-Vin Chang
Department of Physical Medicine and Rehabilitation,
National Taiwan University Hospital Bei-Hu Branch,
87, Nei-Jiang Rd.,
Wan-Hwa District,
Taipei 108, Taiwan
E-mail: kvchang011@gmail.com
Phone: +886223717101-5309

To the Editor,

The occipital nerve (LON) is part of the superficial cervical plexus and originates from the ventral rami of C2 and C3 nerve roots [1,2]. An anatomical study has proposed the possibility of it being compressed not only by the occipital artery branch, but also by the fascial attachment of the sternocleidomastoid muscle and the facial band [3].

Technically, the point where the greater auricular nerve loops around the posterior edge of the sternocleid-

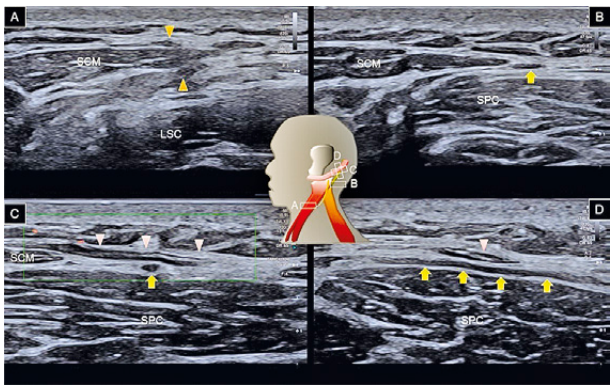

Fig 1. Placing the transducer at the midpoint of the lateral neck border, the greater auricular nerve (dark yellow arrowheads) is seen looping around the posterior edge of the sternocleidomastoid (SCM) muscle (A). The lesser occipital nerve (LON, yellow arrows) emerges from the posterior edge of the SCM muscle and runs cranially and posteriorly on the splenius capitis (SPC) muscle (B). By further shifting the transducer cranially, the transversus nuchae muscle (red arrowheads) may become visible over the LON (C). Rotating the transducer to align with the long axis of the LON reveals the potential entrapment point between the transversus nuchae and the SPC muscles (D). LSC, levator scapular muscle.

omastoid muscle is identified as the punctum nervosum (fig 1A). Moving the transducer cranially allows for visualization of the greater auricular nerve coursing anteriorly and superficially to the sternocleidomastoid muscle. Simultaneously, the LON emerges from the posterior edge of the sternocleidomastoid muscle and runs posteriorly on the splenius capitis muscle (fig 1B).

By further shifting the transducer cranially, a hypoechoic linear structure may become visible over the LON. Power Doppler imaging can be utilized to distinguish this structure from the occipital artery branch (fig 1C; Video 1, on the journal site). The hypoechoic linear structure can be followed anteriorly until it reaches the fascia superficial to the parotid gland and posteriorly to the trapezius fascia and the lateral border of the superior nuchal line, validating it as the transversus nuchae muscle. The muscle has been described to begin at the fascia encircling the external occipital protuberance, proceeds diagonally downward to the apex of the mastoid process, and subsequently extends upward into the cheek area as part of the superficial musculo-aponeurotic system [4]. Rotating the transducer to align with the long axis of the LON reveals the potential entrapment point between the transversus nuchae and splenius capitis muscles (fig 1D). Therefore, in the case of suspected LON entrapment, the LON evaluation should be extended to the level of the transversus nuchae muscle, whereby sono-palpation of the muscle can also be beneficial in eliciting nerve compression symptoms.

Acknowledgment

This study was funded by the National Taiwan University Hospital, Bei-Hu Branch; Ministry of Science and Technology, Taiwan (MOST 106-2314-B-002-180-MY3 and MOST 109-2314-B-002-114-MY3) and National Science and Technology, Taiwan (NSTC 112-2314-B-002-134).

References

1. Chang KV, Lin CP, Hung CY, Özçakar L, Wang TG, Chen WS. Sonographic Nerve Tracking in the Cervical Region: A Pictorial Essay and Video Demonstration. Am J Phys Med Rehabil 2016;95:862-870.
2. Picasso R, Zaottini F, Pistoia F, et al. High-Resolution Ultrasound of Small Clinically Relevant Nerves Running Across the Posterior Triangle of the Neck. Semin Musculoskelet Radiol 2020;24:101-112.
3. Lee M, Brown M, Chepla K, et al. An anatomical study of the lesser occipital nerve and its potential compression points: implications for surgical treatment of migraine headaches. Plast Reconstr Surg 2013;132:1551-1556.
4. Lei T, Cui L, Zhang YZ, et al. Anatomy of the transversus nuchae muscle and its relationship with the superficial musculoaponeurotic system. Plast Reconstr Surg 2010;126:1058-1062.